IEEE Access
Multidisciplinary | Rapid Review | Open Access Journal

Received December 27, 2018, accepted January 21, 2019, date of publication January 25, 2019, date of current version May 29, 2019.

Digital Object Identifier 10.1109/ACCESS.2019.2895314

Hybrid Precoder and Combiner Design for Single-User mmWave MIMO Systems

RAN ZHANG[1], WEIXIA ZOU[1,2], YE WANG[1], AND MINGYANG CUI[1]
[1]Key Lab of Universal Wireless Communications, MOE, Beijing University of Posts and Telecommunications, Beijing 100876, China
[2]State Key Laboratory of Millimeter Waves, Southeast University, Nanjing 210096, China

Corresponding author: Weixia Zou (e-mail: zwx0218@bupt.edu.cn)

This work was supported in part by the NSFC under Grant 61571055, in part by the SKL of MMW under Grant K201815, and in part by the Important National Science and Technology Specific Projects under Grant 2017ZX03001028.

ABSTRACT Millimeter wave (mmWave) communications have been regarded as a key technology for the next generation cellular systems since the huge available bandwidth can potentially provide the rates of multiple gigabits per second. In mmWave multiple-input multiple-output (MIMO) systems, the conventional precoding is infeasible due to the hardware cost and power consumption. Therefore, hybrid precoding is considered as a promising technology to provide a compromise between hardware complexity and system performance. In this paper, we investigate the designs of the hybrid precoder and combiner in mmWave MIMO systems. We adopt the hierarchical strategy to design a hybrid precoder to maximize the spectral efficiency. In particular, we focus on the optimization of analog precoder and propose a novel iterative algorithm. Then, based on the optimal analog precoder, we compute the digital precoder to improve the spectral efficiency. For practical implementation, the proposed hybrid precoder design can be used in wideband systems with orthogonal frequency division multiplexing modulation. The simulation results and mathematical analysis show that the proposed algorithm can achieve near-optimal performance with low complexity for mmWave MIMO systems.

INDEX TERMS Millimeter wave, MIMO, hybrid precoder, iterative optimization, wideband.

I. INTRODUCTION

With the rapid development of wireless devices, many emerging applications, such as artificial intelligence, virtual reality, big data analytics and augmented reality, have entered our life [1]. Meanwhile, the corresponding data traffic has exponentially increased in wireless networks. In order to meet future traffic demands, academia and industry are committed to develop the next generation wireless local area network (WLAN) and mobile cellular communication [2]–[5]. Millimeter wave, whose spectrum is from 30GHz to 300GHz, has recently attracted the attention [6], [7]. However, mmWave signals experience severe propagation loss compared with current cellular bands, due to the atmospheric attenuation, rain fading and low penetration. Thanks to the small wavelength of mmWave, it is feasible to pack a large number of antennas in the same physical dimension. Large-scale antenna arrays can provide beamforming gains to overcome the propagation loss, and synthesize highly directional beams [8]. It also enables simultaneous transmission of multiple data streams resulting in significant improvements to spectral efficiency.

In traditional MIMO systems, the full-digital precoding is completely performed in digital domain, which can control both the magnitudes and phases of signals. However, the full-digital precoding requires dedicated radio frequency (RF) chain for each antenna element. For mmWave MIMO systems with large-scale antenna arrays, the high cost and power consumption of RF chains make full-digital precoding infeasible [9]. To tackle the above issue, hybrid precoding architecture is proposed, which only requires a small number of RF chains between a low-dimensional digital precoder and a high-dimensional analog precoder [10].

Hybrid precoding has received considerable attention to improve the system performance in mmWave MIMO systems. For early work on hybrid precoding design, [11] points out that maximizing the spectral efficiency can be approximated by minimizing the Euclidean distance between hybrid precoder and the full-digital precoder. This operation makes the hybrid precoder design become a matrix factorization

The associate editor coordinating the review of this manuscript and approving it for publication was Avishek Guha.

problem, which, however, is hard to solve due to the hardware constraints of analog components. Exploiting the sparse-scattering characteristics of mmWave channels, [12]–[14] study the codebook-based hybrid precoder design, and the corresponding analog parts are selected from predefined dictionary, such as array response vectors or discrete Fourier transform (DFT) beamformers. Reference [13] proposes an orthogonal matching pursuit (OMP) algorithm, which offers reasonably good performance. In addition, [15] proposes an iterative algorithm based on the OMP algorithm to design hybrid percoder. To reduce the complexity of the OMP algorithm, [16] proposes a partially updated algorithm to design hybrid precoder.

While computing the digital precoder is relatively simple, the main difficulty of designing the hybrid precoder is the analog part with unit modulus constraints [5], [10]. To overcome this difficulty, [17] proposes an alternate optimization algorithm by using matrix decomposition. In particular, this analog precoder is designed by applying the interior-point method in [17]. Reference [18] proposes a coordinate descent method (CDM) algorithm. In this CDM algorithm, the author turns the optimization problem into a simple form, and then derives the closed-form expression to design analog precoder. Reference [19] proposes a heuristic algorithm to design the analog and digital precoder. In addition, the work in [20] proposes two alternating minimization algorithm for the fully-connected structure. The first one is a manifold optimization based alternating minimization (MO-AltMin) algorithm. This algorithm does not need any pre-determined codebook and attempt to directly solve the hybrid precoding problem under the unit modulus constraints. However, due to the large-size antenna array, the number of unit modulus constraints may be substantially large, which leads to the high computational complexity for MO-AltMin algorithm. Thus, [20] proposes an AltMin algorithm using phase extraction (PE-AltMin). This algorithm has lower computational complexity, but it also cause some performance loss. In addition, some references consider to jointly design hybrid precoder and combiner for mmWave MIMO systems. Reference [21] proposes an iterative phase matching algorithm to design hybrid precoder and combiner. In this algorithm, the analog precoder and combiner are implemented by low-resolution phase shifters. Reference [22] proposes a codebook-based joint hybrid precoder and combiner design for multi-stream transmission in mmWave MIMO systems.

For wideband orthogonal frequency division multiplexing (OFDM) systems, the MO-AltMin and PE-AltMin algorithms can also be applied. In addition, based on Gram-Schmidt orthogonalization, [23] proposes a hybrid precoding algorithm for wideband mmWave system with a limited feedback channel. Reference [24] proposes a heuristic algorithm to design hybrid precoder design for single-user and multi-user mmWave systems.

In this paper, we investigate the hybrid precoder and combiner design in mmWave MIMO systems. In particular, instead of minimizing the Euclidean distance between hybrid precoder and the full-digital precoder, we design the hybrid precoder by directly maximizing spectral efficiency aiming to achieve near-optimal performance with low complexity. Thus, we propose an iterative hierarchical hybrid precoding (HHP-Iterative) algorithm to design analog and digital precoder, both in narrowband and wideband mmWave systems. The contributions of this paper are summarized as follows:

- *To simplify the hybrid precoder design, we adopt a hierarchical strategy to divide hybrid precoding optimization problem into analog and digital parts. In this strategy, we first design the optimal analog precoder. Then, with the analog precoder fixed, we compute the optimal digital precoder to improve the spectral efficiency.*
- *Due to the unit modulus constraints, we focus on the analog precoder design. We decompose the optimization problem of analog precoder into a series of sub-problems, and then derive the closed-form solution for each sub-problem. In addition, the results demonstrate that the proposed HHP-Iterative algorithm can achieve near-optimal performance, and enjoy low computational complexity in mmWave MIMO systems.*
- *The proposed HHP-Iterative algorithm can also be used in wideband systems. Simulation results show that the proposed algorithm achieves satisfactory performance in wideband mmWave systems and outperforms the existing OMP and PE-AltMin algorithms.*

The rest of this paper is organized as follows. We present the system, channel model and the problem formulation in Section II. The designs of hybrid precoder and combiner are investigated in Section III. We show that the proposed algorithm can be used for wideband mmWave systems in Section IV. The computational complexity of proposed algorithm is analyzed in Section V. In Section VI, we present the simulation results. Finally, the conclusion of this paper is shown in Section VII.

The following notations are used throughout this paper. $\mathbf{A}$ is a matrix and $\mathbf{a}$ is a column vector. $\mathbf{a}(i)$ is the i-th element of $\mathbf{a}$. $\mathbf{A}(i,j)$ denotes the element of the i-th row and the j-th column of matrix $\mathbf{A}$. $(\cdot)^T$ and $(\cdot)^H$ denote the transpose and transpose-conjugate operations, respectively. $\mathbf{I}_N$ is the $N \times N$ identity matrix. $\det(\mathbf{A})$ denotes the determinant of matrix $\mathbf{A}$. $\mathrm{Tr}(\mathbf{A})$ represents the trace of matrix $\mathbf{A}$. $\mathbb{E}\{\cdot\}$ represents statistical expectation. $\Re\{\cdot\}$ is the real part of a complex number. Finally, $\mathcal{CN}(0,\sigma^2)$ represents the zero-mean complex Gaussian distribution with variance σ^2.

II. SYSTEM MODEL AND PROBLEM FORMULATION

In this section, we present the system model and channel model, and then formulate the hybrid precoding problem.

A. SYSTEM MODEL

Consider a single-user mmWave MIMO system as shown in Fig. 1, where the transmitter uses N_{t} antennas and $N_{\mathrm{RF}}^{\mathrm{t}}$ RF chains to simultaneously transmit N_{s} data streams to the

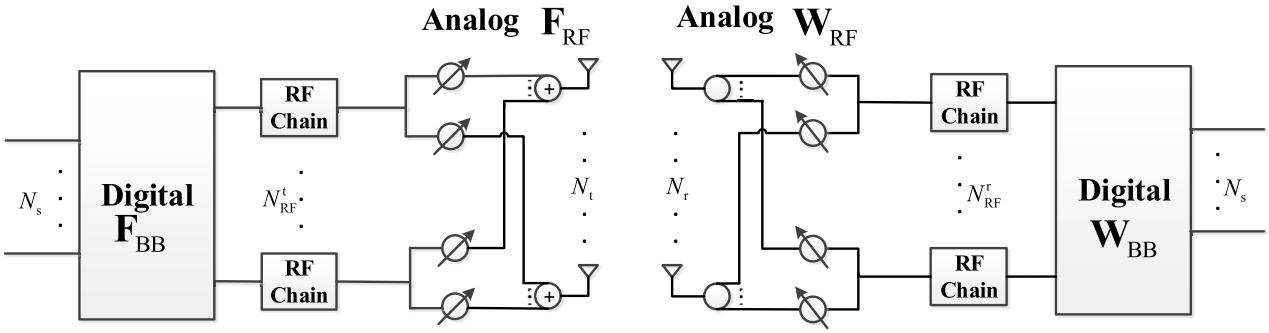

FIGURE 1. A hybrid precoding structure in mmWave MIMO systems.

receiver which is equipped with N_{r} antennas and $N_{\mathrm{RF}}^{\mathrm{r}}$ RF chains. We assume that $N_{\mathrm{RF}}^{\mathrm{t}} = N_{\mathrm{RF}}^{\mathrm{r}} = N_{\mathrm{s}}$ to support such a multi-stream transmission while reducing the energy cost of the mmWave MIMO system.

In Fig.1, the transmitted symbols are processed by an $N_{\mathrm{RF}}^{\mathrm{t}} \times N_{\mathrm{s}}$ digital precoder $\mathbf{F}_{\mathrm{BB}}$, and up-converted to the RF domain via $N_{\mathrm{RF}}^{\mathrm{t}}$ RF chains. Then, the symbols are precoded by an $N_{\mathrm{t}} \times N_{\mathrm{RF}}^{\mathrm{t}}$ analog precoder $\mathbf{F}_{\mathrm{RF}}$. Therefore, the processed signal can be written as

$$\mathbf{x} = \mathbf{F}_{\mathrm{RF}}\mathbf{F}_{\mathrm{BB}}\mathbf{s}, \tag{1}$$

where $\mathbf{s}$ is the $N_{\mathrm{s}} \times 1$ symbol vector such that $\mathbb{E}[\mathbf{s}\mathbf{s}^H] = \frac{1}{N_{\mathrm{s}}}\mathbf{I}_{N_{\mathrm{s}}}$. In addition, the digital precoder enables both amplitude and phase modifications. The analog precoder is implemented by a set of variable phase shifters (PSs), so the elements of $\mathbf{F}_{\mathrm{RF}}$ have constant amplitude, namely $|\mathbf{F}_{\mathrm{RF}}(i,j)| = 1$. Moreover, the transmit power constraint is $\|\mathbf{F}_{\mathrm{RF}}\mathbf{F}_{\mathrm{BB}}\|_F^2 = N_{\mathrm{s}}$.

We consider a narrowband block-fading mmWave channel as in [10], which yields a received signal

$$\mathbf{y} = \sqrt{\rho}\mathbf{H}\mathbf{F}_{\mathrm{RF}}\mathbf{F}_{\mathrm{BB}}\mathbf{s} + \mathbf{n}, \tag{2}$$

where $\mathbf{y}$ is the $N_{\mathrm{r}} \times 1$ received vector, ρ is the average received power, and $\mathbf{n}$ is the noise vector of independent and identically distributed (i.i.d) $\mathcal{CN}(0, \sigma_{\mathrm{n}}^2)$ elements. $\mathbf{H}$ is the $N_{\mathrm{r}} \times N_{\mathrm{t}}$ channel matrix such that $\mathbb{E}[\|\mathbf{H}\|_F^2] = N_{\mathrm{t}}N_{\mathrm{r}}$. Besides, we assume that the channel state information (CSI) of $\mathbf{H}$ is known perfectly at both the transmitter and receiver.

At the receiver, an $N_{\mathrm{r}} \times N_{\mathrm{RF}}^{\mathrm{r}}$ analog combiner $\mathbf{W}_{\mathrm{RF}}$ and an $N_{\mathrm{RF}}^{\mathrm{r}} \times N_{\mathrm{s}}$ digital combiner $\mathbf{W}_{\mathrm{BB}}$ are used to process the received signal. Therefore, the received signal after combining is given as

$$\bar{\mathbf{y}} = \sqrt{\rho}\mathbf{W}_{\mathrm{BB}}^H\mathbf{W}_{\mathrm{RF}}^H\mathbf{H}\mathbf{F}_{\mathrm{RF}}\mathbf{F}_{\mathrm{BB}}\mathbf{s} + \mathbf{W}_{\mathrm{BB}}^H\mathbf{W}_{\mathrm{RF}}^H\mathbf{n}. \tag{3}$$

Similarly to the analog precoder, the analog combiner is also implemented by using phase shifters and satisfies unit modulus constraint, that is $|\mathbf{W}_{\mathrm{RF}}(i,j)| = 1$. When Gaussian signal is transmitted over the mmWave channel, the spectral efficiency achieved is given by [25]

$$R = \log_2 \det\big(\mathbf{I}_{N_{\mathrm{s}}} + \frac{\rho}{N_{\mathrm{s}}}\mathbf{R}_{\mathrm{n}}^{-1}\mathbf{W}_{\mathrm{BB}}^H\mathbf{W}_{\mathrm{RF}}^H\mathbf{H}\mathbf{F}_{\mathrm{RF}}\mathbf{F}_{\mathrm{BB}} \times \mathbf{F}_{\mathrm{BB}}^H\mathbf{F}_{\mathrm{RF}}^H\mathbf{H}^H\mathbf{W}_{\mathrm{RF}}\mathbf{W}_{\mathrm{BB}}\big), \tag{4}$$

where $\mathbf{R}_{\mathrm{n}} = \sigma_{\mathrm{n}}^2\mathbf{W}_{\mathrm{BB}}^H\mathbf{W}_{\mathrm{RF}}^H\mathbf{W}_{\mathrm{RF}}\mathbf{W}_{\mathrm{BB}}$ is the noise covariance matrix after combining.

B. PROBLEM FORMULATION

For single-user mmWave MIMO systems, we aim to jointly design hybrid precoder and combiner to maximize the spectral efficiency. Under hardware constraint, the corresponding problem can be written as

$$\begin{aligned} &\underset{\mathbf{F}_{\mathrm{BB}},\mathbf{F}_{\mathrm{RF}},\mathbf{W}_{\mathrm{BB}},\mathbf{W}_{\mathrm{RF}}}{\arg\max} \quad R \\ &\text{s.t.} \begin{cases} \|\mathbf{F}_{\mathrm{RF}}\mathbf{F}_{\mathrm{BB}}\|_F^2 = N_{\mathrm{s}}, & \\ |\mathbf{F}_{\mathrm{RF}}(i,j)| = 1, & \forall i,j, \\ |\mathbf{W}_{\mathrm{RF}}(i,j)| = 1, & \forall i,j. \end{cases} \end{aligned} \tag{5}$$

This optimization problem is a joint optimization over the hybrid precoder and combiner. However, it is difficult to be solved due to the non-convex constraint on analog precoder and combiner. In the following section, we attempt to simplify the objective problem and achieve a satisfactory performance.

C. MILLIMETER WAVE CHANNEL MODEL

In mmWave systems, due to the high path loss at mmWave band and tightly packed antenna arrays lead to limited scattering and high antenna correlation. We adopt a narrowband clustered mmWave channel model based on the extended Saleh-Valenzuela model [26]. The matrix channel $\mathbf{H}$ is assumed to have N_{cl} scattering clusters, each of which contains N_{ray} propagation paths [13], [20]. Therefore, the channel $\mathbf{H}$ can be written as

$$\mathbf{H} = \gamma \sum_{i=1}^{N_{\mathrm{cl}}}\sum_{l=1}^{N_{\mathrm{ray}}} \alpha_{il}\mathbf{a}_{\mathrm{r}}(\phi_{il}^{\mathrm{r}}, \theta_{il}^{\mathrm{r}})\mathbf{a}_{\mathrm{t}}(\phi_{il}^{\mathrm{t}}, \theta_{il}^{\mathrm{t}})^H, \tag{6}$$

where γ is a normalization factor such as $\gamma = \sqrt{\frac{N_{\mathrm{t}}N_{\mathrm{r}}}{N_{\mathrm{cl}}N_{\mathrm{ray}}}}$. α_{il} is the complex gain of the l-th ray in the i-th scattering cluster. We assume that α_{il} are i.i.d. random variables following the complex Gaussian distribution $\mathcal{CN}(0, \sigma_{\alpha,i}^2)$, and $\sum_{i=1}^{N_{\mathrm{cl}}}\sigma_{\alpha,i}^2 = \gamma$. In addition, the vectors $\mathbf{a}_{\mathrm{r}}(\phi_{il}^{\mathrm{r}}, \theta_{il}^{\mathrm{r}})$ and $\mathbf{a}_{\mathrm{t}}(\phi_{il}^{\mathrm{t}}, \theta_{il}^{\mathrm{t}})$ are the receive and transmit array response vectors, where $\phi_{il}^{\mathrm{r}}(\theta_{il}^{\mathrm{r}})$ and $\phi_{il}^{\mathrm{t}}(\theta_{il}^{\mathrm{t}})$ stand for azimuth and elevation angles of arrival and departure (AoAs and AoDs), respectively. In this case of a

uniform planar array (UPA) in the $yz-plane$[2] with W and H elements on the y and z axes respectively, the array response vector is given by

$$\mathbf{a}_{\mathrm{UPA}}(\phi,\theta)=\frac{1}{\sqrt{N}}[1,\cdots,e^{jkd(m\sin(\phi)\sin(\theta)+n\cos(\theta))},\cdots,e^{jkd((W-1)\sin(\phi)\sin(\theta)+(H-1)\cos(\theta))}]^T, \quad (7)$$

where d is the antenna spacing, $k=\frac{2\pi}{\lambda}$ and λ is the signal wavelength, and $0\le m\le W$ and $0\le n\le H$ are the antenna indices in 2D plan and the antenna array size is $N=WH$.

III. HIERARCHICAL HYBRID PRECODER AND COMBINER DESIGN

In this section, we first consider to design hybrid precoder and propose the HHP-Iterative algorithm to obtain the optimal analog precoder and digital precoder in Section III.A. Then, since the hybrid combiner and precoder have similar architecture and mathematical formulations, we can use the proposed algorithm to design hybrid combiner in Section III.B.

A. HYBRID PRECODER DESIGN

We seek to design hybrid precoder that maximize the spectral efficiency of transceiver in (5). However, this problem involves joint optimization over the hybrid precoder and combiner, which is difficult to solve. In order to simplify transceiver design, we temporarily decouple the joint transmitter-receiver optimization problem and focus on the hybrid precoder design. Thus, according to [13], we design hybrid precoder by maximizing the mutual information achieved by Gaussian signal over the mmWave channel to improve the spectral efficiency. The corresponding hybrid precoder problem can be formulate as

$$\begin{aligned}&\arg\max_{\mathbf{F}_{\mathrm{BB}},\mathbf{F}_{\mathrm{RF}}}\ \log_2\det\Big(\mathbf{I}+\frac{\rho}{N_{\mathrm{s}}\sigma_{\mathrm{n}}^2}\mathbf{H}\mathbf{F}_{\mathrm{RF}}\mathbf{F}_{\mathrm{BB}}\mathbf{F}_{\mathrm{BB}}^H\mathbf{F}_{\mathrm{RF}}^H\mathbf{H}^H\Big)\\&\text{s.t.}\ \begin{cases}\|\mathbf{F}_{\mathrm{RF}}\mathbf{F}_{\mathrm{BB}}\|_F^2=N_{\mathrm{s}}, & \forall i,j,\\ |\mathbf{F}_{\mathrm{RF}}(i,j)|=1, & \forall i,j.\end{cases}\end{aligned} \quad (8)$$

Obviously, due to the unit modulus constraint of $\mathbf{F}_{\mathrm{RF}}$, jointly optimizing $\mathbf{F}_{\mathrm{BB}}$ and $\mathbf{F}_{\mathrm{RF}}$ is intractable. Inspired in [19] and [27], we adopt a hierarchical strategy to design digital and analog precoder. In the first part, we employ the water-filling method to design the optimal $\mathbf{F}_{\mathrm{BB}}$, assuming that the analog precoder is fixed. In the second part, based on the optimal digital precoder, we focus on design analog precoder. Then, we decompose the analog precoder optimization problem into a series of sub-problems and propose an iterative algorithm, which designs each element of $\mathbf{F}_{\mathrm{RF}}$ successively until convergence.

1) DIGITAL PRECODER DESIGN

Assuming that the analog precoder is fixed, we consider the digital precoder design to improve the spectral efficiency. To further simplify hybrid precoder design and decouple the digital and analog precoder in the power constraint, we set $\mathbf{F}_{\mathrm{BB}}=(\mathbf{F}_{\mathrm{RF}}^H\mathbf{F}_{\mathrm{RF}})^{-\frac{1}{2}}\tilde{\mathbf{F}}_{\mathrm{BB}}$ with $\tilde{\mathbf{F}}_{\mathrm{BB}}$ a dummy variable, and then bring $\mathbf{F}_{\mathrm{BB}}$ into (8). Therefore, the digital precoder design problem in (8) can be rewritten as

$$\begin{aligned}&\arg\max_{\tilde{\mathbf{F}}_{\mathrm{BB}}}\ \log_2\det\Big(\mathbf{I}+\frac{\rho}{N_{\mathrm{s}}\sigma_{\mathrm{n}}^2}\mathbf{H}_{\mathrm{e}}\tilde{\mathbf{F}}_{\mathrm{BB}}\tilde{\mathbf{F}}_{\mathrm{BB}}^H\mathbf{H}_{\mathrm{e}}^H\Big)\\&\text{s.t.}\ \|\tilde{\mathbf{F}}_{\mathrm{BB}}\|_F^2=N_{\mathrm{s}},\end{aligned} \quad (9)$$

where $\mathbf{H}_{\mathrm{e}}=\mathbf{H}\mathbf{F}_{\mathrm{RF}}(\mathbf{F}_{\mathrm{RF}}^H\mathbf{F}_{\mathrm{RF}})^{-\frac{1}{2}}$ is defined as an effective channel. This objective function and constraint in (9) only have one optimization variable $\tilde{\mathbf{F}}_{\mathrm{BB}}$. Thus, we can easily use the water-filling method to design $\tilde{\mathbf{F}}_{\mathrm{BB}}$. The corresponding solution of $\tilde{\mathbf{F}}_{\mathrm{BB}}$ is given as

$$\tilde{\mathbf{F}}_{\mathrm{BB}}=\mathbf{V}_{\mathrm{e}}\mathbf{P}_{\mathrm{e}}, \quad (10)$$

where $\mathbf{V}_{\mathrm{e}}$ is the first N_{s} columns of right singular vectors of $\mathbf{H}_{\mathrm{e}}$. $\mathbf{P}_{\mathrm{e}}$ is a diagonal matrix whose diagonal elements are the water-filling power control solution. If the optimal $\tilde{\mathbf{F}}_{\mathrm{BB}}$ is found, the optimal digital precoder can be obtained by

$$\begin{aligned}\mathbf{F}_{\mathrm{BB}}&=(\mathbf{F}_{\mathrm{RF}}^H\mathbf{F}_{\mathrm{RF}})^{-\frac{1}{2}}\tilde{\mathbf{F}}_{\mathrm{BB}}\\&=(\mathbf{F}_{\mathrm{RF}}^H\mathbf{F}_{\mathrm{RF}})^{-\frac{1}{2}}\mathbf{V}_{\mathrm{e}}\mathbf{P}_{\mathrm{e}}.\end{aligned} \quad (11)$$

2) ANALOG PRECODER DESIGN

For the optimal digital precoder, we focus on the analog precoder design to maximize the spectral efficiency. In particular, it has been verified in [19] that the analog precoder satisfies $\mathbf{F}_{\mathrm{RF}}^H\mathbf{F}_{\mathrm{RF}}\propto\mathbf{I}$ with high probability when the number of antennas tends to infinity. This enables us to obtain $\mathbf{F}_{\mathrm{BB}}=(\mathbf{F}_{\mathrm{RF}}^H\mathbf{F}_{\mathrm{RF}})^{-\frac{1}{2}}\mathbf{V}_{\mathrm{e}}\mathbf{P}_{\mathrm{e}}\approx\mathbf{V}_{\mathrm{e}}\mathbf{P}_{\mathrm{e}}$. In addition, $\mathbf{V}_{\mathrm{e}}$ is a unitary matrix for the case that the number of RF chains is equal to that of the data streams. $\mathbf{P}_{\mathrm{e}}\approx\mu\mathbf{I}$, where μ is a normalization factor, assuming that equal power allocation for all data streams. So, we can obtain $\mathbf{F}_{\mathrm{BB}}\mathbf{F}_{\mathrm{BB}}^H\approx\mu^2\mathbf{I}$. Then, we can rewrite the optimization problem (8) as

$$\begin{aligned}&\arg\max_{\mathbf{F}_{\mathrm{RF}}}\ \log_2\det\Big(\mathbf{I}+\frac{\rho\mu^2}{N_{\mathrm{s}}\sigma_{\mathrm{n}}^2}\mathbf{H}\mathbf{F}_{\mathrm{RF}}\mathbf{F}_{\mathrm{RF}}^H\mathbf{H}^H\Big)\\&\text{s.t.}\ |\mathbf{F}_{\mathrm{RF}}(i,j)|=1,\quad\forall i,j.\end{aligned} \quad (12)$$

Since the column permutation of $\mathbf{F}_{\mathrm{RF}}$ does not change the result of $\mathbf{F}_{\mathrm{RF}}\mathbf{F}_{\mathrm{RF}}^H$, $\mathbf{F}_{\mathrm{RF}}\mathbf{F}_{\mathrm{RF}}^H$ can be rewritten as

$$\mathbf{F}_{\mathrm{RF}}\mathbf{F}_{\mathrm{RF}}^H=\big[(\mathbf{F}_{\mathrm{RF}})_{-j}\,\mathbf{f}_j\big]\big[(\mathbf{F}_{\mathrm{RF}})_{-j}\,\mathbf{f}_j\big]^H, \quad (13)$$

where $(\mathbf{F}_{\mathrm{RF}})_{-j}$ is a sub-matrix of $\mathbf{F}_{\mathrm{RF}}$ excluding the j-th column $\mathbf{f}_j$. Therefore, the objective function of (12) can be equivalent to (14), as shown at the bottom of the next page, which is presented at the bottom of next page, where we define the auxiliary matrix $\mathbf{Q}_j$ as

$$\mathbf{Q}_j=\mathbf{I}+\frac{\rho\mu^2}{N_{\mathrm{s}}\sigma_{\mathrm{n}}^2}\mathbf{H}(\mathbf{F}_{\mathrm{RF}})_{-j}(\mathbf{F}_{\mathrm{RF}})_{-j}^H\mathbf{H}^H. \quad (15)$$

In (14), selecting appropriate initial matrix $\mathbf{F}_{\mathrm{RF}}$ and assuming that $(\mathbf{F}_{\mathrm{RF}})_{-j}$ is fixed, we can decompose the analog precoder optimization problem into a series of sub-problems.

The j-th optimization sub-problem can be written as

$$\begin{aligned} &\arg\max_{\mathbf{f}_j} \ \log_2\det\Big(1+\frac{\rho\mu^2}{N_s\sigma_n^2}\mathbf{f}_j^H\mathbf{H}^H\mathbf{Q}_j^{-1}\mathbf{H}\mathbf{f}_j\Big)\\ &\text{s.t. } |\mathbf{f}_j|=1, \quad \forall j. \end{aligned} \tag{16}$$

We notice that maximizing problem (16) over $\mathbf{f}_j$ can be equivalent to

$$\begin{aligned} &\arg\max_{\mathbf{f}_j} \ \big|\mathbf{f}_j^H\mathbf{H}^H\mathbf{Q}_j^{-1}\mathbf{H}\mathbf{f}_j\big|\\ &\text{s.t. } |\mathbf{f}_j|=1, \quad \forall j. \end{aligned} \tag{17}$$

To easily solve this problem, we define an intermediate matrix $\mathbf{M}_j=\mathbf{H}^H\mathbf{Q}_j^{-1}\mathbf{H}$. In addition, we use $\mathbf{f}_j(i)$ to represent the i-th element of $\mathbf{f}_j$. Thus, each element of $\mathbf{f}_j$ can be iteratively obtained by the following *Proposition 1*, whose proof is provided in Appendix A.

Proposition 1: Given the elements of analog precoder $\{\mathbf{f}_j(1),\mathbf{f}_j(2),\cdots,\mathbf{f}_j(u),\cdots,\mathbf{f}_j(N_t)\}$, $u\neq i$, the optimal solution of $\mathbf{f}_j(i)$ is

$$\mathbf{f}_j^{\text{opt}}(i)=\psi\Big\{\sum_{\substack{u=1\\u\neq i}}^{N_t}\mathbf{M}_j^H(u,i)\mathbf{f}_j(u)\Big\}, \tag{18}$$

where for the complex variable x,

$$\psi(x)=\begin{cases}1, & x=0\\ \frac{x}{|x|}, & x\neq 0.\end{cases} \tag{19}$$

Note that we can obtain the optimal solution $\mathbf{f}_j^{\text{opt}}(i)$ by the *Proposition 1*. However, we need to compute the matrices $\mathbf{Q}_j$ and $\mathbf{M}_j=\mathbf{H}^H\mathbf{Q}_j^{-1}\mathbf{H}$, which lead to high computation complexity. Specifically, by some standard mathematical operations, the computation of $\mathbf{M}_j$ can be significantly simplified as shown in the following *Proposition 2*, whose proof is provided in Appendix B.

Proposition 2: The matrix $\mathbf{M}_j=\mathbf{H}^H\mathbf{Q}_j^{-1}\mathbf{H}$, where $\mathbf{Q}_j=\mathbf{I}+\frac{\rho\mu^2}{N_s\sigma_n^2}\mathbf{H}(\mathbf{F}_{\text{RF}})_{-j}(\mathbf{F}_{\text{RF}})_{-j}^H\mathbf{H}^H$, can be simplified as

$$\mathbf{M}_j=\mathbf{B}+\frac{\frac{\rho\mu^2}{N_s\sigma_n^2}\mathbf{B}\mathbf{f}_j\mathbf{f}_j^H\mathbf{B}}{1-\frac{\rho\mu^2}{N_s\sigma_n^2}\mathbf{f}_j^H\mathbf{B}\mathbf{f}_j}, \tag{20}$$

where the matrix $\mathbf{B}=\mathbf{H}^H\mathbf{A}^{-1}\mathbf{H}$ and the matrix $\mathbf{A}=\mathbf{I}+\frac{\rho\mu^2}{N_s\sigma_n^2}\mathbf{H}\mathbf{F}_{\text{RF}}\mathbf{F}_{\text{RF}}^H\mathbf{H}^H$.

Algorithm 1 Hierarchical Hybrid Precoding Based on Iterative Algorithm (HHP-Iterative)

Input: $\mathbf{H}$, $\mathbf{B}$, N_t, N_s, ρ, μ

Construct $\mathbf{F}_{\text{RF}}^{(0)}$ with random phases and set $k=0$;
repeat
  for $j=1:N_s$ **do**
    Obtain $\mathbf{f}_j$ from $\mathbf{F}_{\text{RF}}^{(k)}$;
    Update $\mathbf{M}_j=\mathbf{B}+\frac{\frac{\rho\mu^2}{N_s\sigma_n^2}\mathbf{B}\mathbf{f}_j\mathbf{f}_j^H\mathbf{B}}{1-\frac{\rho\mu^2}{N_s\sigma_n^2}\mathbf{f}_j^H\mathbf{B}\mathbf{f}_j}$;
    while no convergence of $\mathbf{f}_j(i)$ **do**
      for $i=1:N_t$ **do**
        $\mathbf{f}_j(i)=\psi\Big\{\sum_{\substack{u=1\\u\neq i}}^{N_t}\mathbf{M}_j^H(u,i)\mathbf{f}_j(u)\Big\}$
      end for
    end while
    Construct $\mathbf{f}_j^{(k+1)}$ by $\{\mathbf{f}_j(i)\}_{i=1}^{N_t}$;
  end for
  Construct $\mathbf{F}_{\text{RF}}^{(k+1)}$ by $\{\mathbf{f}_j^{(k+1)}\}_{j=1}^{N_s}$;
  $k\leftarrow k+1$;
until A stopping criterion triggers;
Compute $\mathbf{F}_{\text{BB}}$ according to (11);

Output: $\mathbf{F}_{\text{BB}}$, $\mathbf{F}_{\text{RF}}$

In (20), the matrix $\mathbf{M}_j$ only involves matrix-to-vector multiplication instead of the complicated matrix inversion and matrix-to-matrix multiplication. In addition, the complexity analysis will be given in Section V.

To better present our strategy, we summarize the proposed HHP-Iterative algorithm in Algorithm 1. In this algorithm, we first select appropriate initial analog precoding matrix, then iteratively design each element of analog precoder until convergence. In fact, each element $\mathbf{f}_j(i)$ only requires a few cycles to reach convergence in our simulation. After that, we compute the digital precoder based on the optimal analog precoder to improve the spectral efficiency.

$$\begin{aligned} &\log_2\det\Big(\mathbf{I}+\frac{\rho\mu^2}{N_s\sigma_n^2}\mathbf{H}\mathbf{F}_{\text{RF}}\mathbf{F}_{\text{RF}}^H\mathbf{H}^H\Big)\\ &=\log_2\det\Big(\mathbf{I}+\frac{\rho\mu^2}{N_s\sigma_n^2}\mathbf{H}\big[\mathbf{F}_{\text{RF}(-j)}\ \mathbf{f}_j\big]\big[\mathbf{F}_{\text{RF}(-j)}\ \mathbf{f}_j\big]^H\mathbf{H}^H\Big)\\ &=\log_2\det\Big(\mathbf{I}+\frac{\rho\mu^2}{N_s\sigma_n^2}\mathbf{H}\mathbf{F}_{\text{RF}(-j)}\mathbf{F}_{\text{RF}(-j)}^H\mathbf{H}^H+\frac{\rho\mu^2}{N_s\sigma_n^2}\mathbf{H}\mathbf{f}_j\mathbf{f}_j^H\mathbf{H}^H\Big)\\ &=\log_2\det\big(\mathbf{Q}_j\big)+\log_2\det\Big(\mathbf{I}+\frac{\rho\mu^2}{N_s\sigma_n^2}\mathbf{Q}_j^{-1}\mathbf{H}\mathbf{f}_j\mathbf{f}_j^H\mathbf{H}^H\Big)=\log_2\det\big(\mathbf{Q}_j\big)+\log_2\det\Big(1+\frac{\rho\mu^2}{N_s\sigma_n^2}\mathbf{f}_j^H\mathbf{H}^H\mathbf{Q}_j^{-1}\mathbf{H}\mathbf{f}_j\Big). \end{aligned} \tag{14}$$

In particular, in HHP-Iterative algorithm, the output of each iteration, i.e. the analog precoding matrix $\mathbf{F}_{\mathrm{RF}}^{(k+1)}$, will become the new input $\mathbf{F}_{\mathrm{RF}}^{(k)}$ for the next iteration until the stopping criterion is reached. In this paper, the stopping criterion is based on the number of iterations. For clarity, we will further analyze the number of iterations in the simulation section.

B. HYBRID COMBINER DESIGN

In this section, we design hybrid combiner to maximize the overall spectral efficiency in (5) when the hybrid precoder are already designed. The corresponding problem formulation is

$$\begin{aligned}&\arg\max_{\mathbf{W}_{\mathrm{BB}},\mathbf{W}_{\mathrm{RF}}}\ \log_2\det\Big(\mathbf{I}+\frac{\rho}{N_{\mathrm{s}}}\mathbf{R}_{\mathrm{n}}^{-1}\mathbf{W}_{\mathrm{BB}}^H\mathbf{W}_{\mathrm{RF}}^H\mathbf{H}_1\mathbf{H}_1^H\times\mathbf{W}_{\mathrm{RF}}\mathbf{W}_{\mathrm{BB}}\Big)\\&\text{s.t. }|\mathbf{W}_{\mathrm{RF}}(i,j)|=1,\quad\forall i,j,\end{aligned}\tag{21}$$

where $\mathbf{H}_1=\mathbf{H}\mathbf{F}_{\mathrm{RF}}\mathbf{F}_{\mathrm{BB}}$. Similarly to the analog precoder, the analog combiner still satisfies $\mathbf{W}_{\mathrm{RF}}^H\mathbf{W}_{\mathrm{RF}}\propto\mathbf{I}$ for large-scale antenna arrays in [19]. Therefore, if we assume $\mathbf{W}_{\mathrm{BB}}\mathbf{W}_{\mathrm{BB}}^H\approx\eta^2\mathbf{I}$, where η^2 is normalization factor, we have $\mathbf{W}_{\mathrm{BB}}^H\mathbf{W}_{\mathrm{RF}}^H\mathbf{W}_{\mathrm{RF}}\mathbf{W}_{\mathrm{BB}}\approx\mathbf{I}$. The objective function in (21) can be approximated as

$$\begin{aligned}&\log_2\det\Big(\mathbf{I}+\frac{\rho}{N_{\mathrm{s}}}\mathbf{R}_{\mathrm{n}}^{-1}\mathbf{W}_{\mathrm{BB}}^H\mathbf{W}_{\mathrm{RF}}^H\mathbf{H}_1\mathbf{H}_1^H\mathbf{W}_{\mathrm{RF}}\mathbf{W}_{\mathrm{BB}}\Big)\\&\quad\approx\log_2\det\Big(\mathbf{I}+\frac{\rho}{N_{\mathrm{s}}\sigma_{\mathrm{n}}^2}\mathbf{W}_{\mathrm{BB}}^H\mathbf{W}_{\mathrm{RF}}^H\mathbf{H}_1\mathbf{H}_1^H\mathbf{W}_{\mathrm{RF}}\mathbf{W}_{\mathrm{BB}}\Big).\end{aligned}\tag{22}$$

According to the proposed hierarchical strategy, we first design the digital combiner for a fixed analog combiner. The digital combiner design problem can be written as

$$\arg\max_{\mathbf{W}_{\mathrm{BB}}}\ \log_2\det\Big(\mathbf{I}+\frac{\rho}{N_{\mathrm{s}}\sigma_{\mathrm{n}}^2}\mathbf{W}_{\mathrm{BB}}^H\mathbf{W}_{\mathrm{RF}}^H\mathbf{H}_1\mathbf{H}_1^H\times\mathbf{W}_{\mathrm{RF}}\mathbf{W}_{\mathrm{BB}}\Big).\tag{23}$$

By singular value decomposition (SVD) of $\mathbf{H}_1^H\mathbf{W}_{\mathrm{RF}}$, i.e. $\mathbf{H}_1^H\mathbf{W}_{\mathrm{RF}}=\mathbf{U}_1\Lambda_1\mathbf{V}_1^H$, the solution of digital combiner design is

$$\mathbf{W}_{\mathrm{BB}}=\mathbf{V}_1.\tag{24}$$

Since $\mathbf{W}_{\mathrm{BB}}$ is an unitary matrix, the previous assumption of $\mathbf{W}_{\mathrm{BB}}\mathbf{W}_{\mathrm{BB}}^H\approx\eta^2\mathbf{I}$ is valid. Then, according to the optimal $\mathbf{W}_{\mathrm{BB}}$, the analog combiner design problem in (21) can be written as

$$\begin{aligned}&\arg\max_{\mathbf{W}_{\mathrm{RF}}}\ \log_2\det\Big(\mathbf{I}+\frac{\rho\eta^2}{N_{\mathrm{s}}\sigma_{\mathrm{n}}^2}\mathbf{H}_1^H\mathbf{W}_{\mathrm{RF}}\mathbf{W}_{\mathrm{RF}}^H\mathbf{H}_1\Big)\\&\text{s.t. }|\mathbf{W}_{\mathrm{RF}}(i,j)|=1,\quad\forall i,j.\end{aligned}\tag{25}$$

This problem of analog combiner happens to have the same form as the problem of analog precoder in (12). Thus, replacing the symbols $\mathbf{F}_{\mathrm{RF}}$ and $\mathbf{H}$ by $\mathbf{W}_{\mathrm{RF}}$ and $\mathbf{H}_1$, Algorithm1 can be directly used to obtain the optimal analog combiner.

IV. HYBRID PRECODER IN WIDEBAND MMWAVE MIMO-OFDM SYSTEMS

For mmWave MIMO-OFDM systems, the signal of each subcarrier first is precoded by a digital precoder. Then the processed signals go through the inverse fast Fourier transform (IFFT) operation. After that, the signals of all the subcarriers are combined together, and then processed by an analog precoder to form the transmitted signal. In particular, since the analog precoding is a post-IFFT process, the analog precoder is same for all the subcarriers [20], [24]. Therefore, after the decoding, the received signal at subcarrier k can be represented as [24]

$$\begin{aligned}\mathbf{y}[k]=&\sqrt{\rho}\mathbf{W}_{\mathrm{BB}}^H[k]\mathbf{W}_{\mathrm{RF}}^H\mathbf{H}[k]\mathbf{F}_{\mathrm{RF}}\mathbf{F}_{\mathrm{BB}}[k]\mathbf{s}[k]\\&+\mathbf{W}_{\mathrm{BB}}[k]\mathbf{W}_{\mathrm{RF}}^H\mathbf{n}[k],\end{aligned}\tag{26}$$

where $\mathbf{H}[k]$ is channel matrix of the k-th subcarrier in mmWave MIMO-OFDM systems [28]. The corresponding channel matrix is given by

$$\mathbf{H}[k]=\gamma\sum_{i=1}^{N_{\mathrm{cl}}-1}\sum_{l=1}^{N_{\mathrm{ray}}}\alpha_{il}\mathbf{a}_{\mathrm{r}}(\phi_{il}^{\mathrm{r}},\theta_{il}^{\mathrm{r}})\mathbf{a}_{\mathrm{t}}(\phi_{il}^{\mathrm{t}},\theta_{il}^{\mathrm{t}})^H e^{-j2\pi ik/K},\tag{27}$$

where K is the number of subcarriers. In wideband mmWave MIMO-OFDM systems, the hybrid precoder design is formulated as [24]

$$\begin{aligned}&\arg\max_{\mathbf{F}_{\mathrm{RF}},\{\mathbf{F}_{\mathrm{BB}}[k]\}_{k=1}^K}\ \frac{1}{K}\sum_{k=1}^{K}\tilde{R}[k]\\&\text{s.t.}\begin{cases}\|\mathbf{F}_{\mathrm{RF}}\mathbf{F}_{\mathrm{BB}}[k]\|_F^2=N_{\mathrm{s}},\\|\mathbf{F}_{\mathrm{RF}}(i,j)|=1,\quad\forall i,j,\end{cases}\end{aligned}\tag{28}$$

where $\tilde{R}[k]=\log_2\det\big(\mathbf{I}+\frac{\rho}{N_{\mathrm{s}}\sigma_{\mathrm{n}}^2}\mathbf{H}[k]\mathbf{F}_{\mathrm{RF}}\mathbf{F}_{\mathrm{BB}}[k]\mathbf{F}_{\mathrm{BB}}^H[k]\mathbf{F}_{\mathrm{RF}}^H\times\mathbf{H}^H[k]\big)$ is the transmitter achievable rate of the k-th subcarrier. Similar to narrowband case in (8), this optimization problem is non-convex and difficult to be solved. Fortunately, the proposed HHP-Iterative framework can be used to design hybrid precoder and solve problem (28) for wideband mmWave MIMO-OFDM systems.

We first design digital precoder for the fixed analog precoder in wideband mmWave MIMO-OFDM systems. Since the digital precoders of all subcarriers operate in parallel, we can remove the summation from (28), and then optimize the digital precoder for each subcarrier. The corresponding problem is

$$\begin{aligned}&\arg\max_{\mathbf{F}_{\mathrm{BB}}[k]}\ \log_2\det\Big(\mathbf{I}+\frac{\rho}{N_{\mathrm{s}}\sigma_{\mathrm{n}}^2}\mathbf{H}[k]\mathbf{F}_{\mathrm{RF}}\mathbf{F}_{\mathrm{BB}}[k]\\&\qquad\times\mathbf{F}_{\mathrm{BB}}^H[k]\mathbf{F}_{\mathrm{RF}}^H\mathbf{H}^H[k]\Big)\\&\text{s.t. }\|\mathbf{F}_{\mathrm{RF}}\mathbf{F}_{\mathrm{BB}}[k]\|_F^2=N_{\mathrm{s}}.\end{aligned}\tag{29}$$

According to the solution in (11), we can obtain the optimal digital precoder of each subcarrier as

$$\mathbf{F}_{\mathrm{BB}}[k]=\Big(\mathbf{F}_{\mathrm{RF}}^H\mathbf{F}_{\mathrm{RF}}\Big)^{-\frac{1}{2}}\mathbf{V}_{\mathrm{e}}[k]\mathbf{P}_{\mathrm{e}}.\tag{30}$$

In (30), the digital precoder still satisfies $\mathbf{F}_{\mathrm{BB}}[k]\mathbf{F}_{\mathrm{BB}}^H[k]\approx\mu^2\mathbf{I}$. In wideband mmWave MIMO-OFDM systems, however, the analog precoder is identical for all subcarriers, which is the primary difference from

narrowband systems. Thus, based on the obtained digital precoder, we simplify problem (28) to design the analog precoder, and the corresponding problem can be converted as

$$\arg\max_{\mathbf{F}_{\mathrm{RF}}} \frac{1}{K}\sum_{k=1}^{K}\log_2\det\Big(\mathbf{I}+\frac{\rho\mu^2}{N_{\mathrm{s}}\sigma_{\mathrm{n}}^2}\mathbf{H}[k]\mathbf{F}_{\mathrm{RF}}\mathbf{F}_{\mathrm{RF}}^H\mathbf{H}^H[k]\Big)$$
$$\text{s.t. } |\mathbf{F}_{\mathrm{RF}}(i,j)|=1,\quad \forall i,j. \tag{31}$$

To solve this problem, we derive an upper-bound of this objective function in (32), as shown at the bottom of this page, which is presented at the bottom of this page. In particular, (b) is obtained by using Jensen's inequality, i.e., for a concave function $f(\cdot)$, if $\sum_i \lambda_i = 1$, then $\sum_i \lambda_i f(\mathbf{X}_i) \le f(\sum_i \lambda_i \mathbf{X}_i)$.

After that, using *Proposition 1*, the optimal solution of analog precoder for wideband mmWave MIMO-OFDM, is given as

$$\mathbf{f}_j^{\mathrm{opt}}(i) = \psi\Big\{\sum_{\substack{u=1\\u\neq i}}^{N_{\mathrm{t}}}\mathbf{Z}_j^H(u,i)\mathbf{f}_j(u)\Big\}, \tag{33}$$

where $\mathbf{Z} = \frac{1}{K}\sum_{k=1}^{K}\mathbf{H}^H[k]\mathbf{Q}_j^{-1}[k]\mathbf{H}[k]$ is defined as an intermediate matrix.

Similarly to the hybrid precoder, the solution of hybrid combiner can also be computed. Therefore, the aforementioned analysis shows that the proposed HHP-Iterative algorithm can be used to wideband mmWave systems.

V. COMPLEXITY ANALYSIS

In this section, the complexity of proposed hybrid precoding design is analyzed in terms of the total number of complex multiplications. Therefore, the complexity mainly comes from the following three parts:

1) The first part originates from the update of $\mathbf{M}_j$. In HHP-Iterative algorithm, there is N_{s} iteration to update matrix $\mathbf{M}_j$. In each iteration, according to *Proposition 2*, we know that the complexity of $\mathbf{M}_j$ is $\mathcal{O}(N_{\mathrm{t}}^2)$. Thus, after N_{s} iteration, the total computational complexity of $\mathbf{M}_j$ becomes $\mathcal{O}(N_{\mathrm{t}}^2 N_{\mathrm{s}})$.

2) The second part is from obtaining the optimal solution of analog precoder. In particular, according to (18), the each element of analog precoder can be computed and the corresponding complexity is $\mathcal{O}(N_{\mathrm{t}})$. In addition, to reach convergence, each element only requires a few cycles in our simulation. Moreover, in HHP-Iterative algorithm, we need to execute $N_{\mathrm{t}}N_{\mathrm{s}}$ iterations to obtain the optimal analog precoder. Therefore, the computational complexity of second part is $\mathcal{O}(N_{\mathrm{t}}^2 N_{\mathrm{s}})$.

3) The last part stems from calculating digital precoder in (11). In particular, it is observed that $\mathbf{V}_{\mathrm{e}}$ is obtained from the SVD of $\mathbf{H}_{\mathrm{e}}$ and the corresponding complexity is $\mathcal{O}(N_{\mathrm{r}}N_s^2)$. Then, according to (11), the computational complexity of last part is $\mathcal{O}(N_{\mathrm{t}}N_s^2 + N_{\mathrm{r}}N_s^2 + 4N_s^3)$.

To sum up, the computational complexity of the proposed algorithm is approximately $\mathcal{O}(N_{\mathrm{t}}^2 N_{\mathrm{s}})$. In the proposed HHP-Iterative algorithm, the analog precoder is designed by computing the closed-form solutions of each element successively, and these solutions are low dimension. In particular, the matrix $\mathbf{M}_j$ is simplified. Thus, the computational complexity of the proposed algorithm is acceptable. By contrast, the computational complexity of the RF-Iterative algorithm [19] is $\mathcal{O}(N_{\mathrm{t}}^3 N_{\mathrm{s}})$. It is obvious that the computational complexity of the proposed algorithm is lower than that of RF-Iterative algorithm.

VI. SIMULATION RESULTS

In this section, we present simulation results of the proposed algorithm under an $N_{\mathrm{r}} \times N_{\mathrm{t}} = 36 \times 144$ mmWave MIMO system. Due to the favorable propagation performance and compact phasical size, the UPA is especially suitable for mmWave MIMO systems [29]. Thus, both transmitter and receiver are equipped with UPA, which is also consistent with reference algorithms in [13] and [20]. Moreover, according to [20], we model the propagation environment as a $N_{\mathrm{cl}} = 5$ cluster environment with $N_{\mathrm{ray}} = 10$ rays per cluster. In addition, the average power of each cluster is $\sigma_{\alpha,i}^2 = 1$. The azimuth and elevation AoDs and AOAs follow the Laplacian distribution with uniformly distributed mean angles over $[0, 2\pi]$ and angular spread of 10°. Moreover, Signal-to-noise ratio is defined as SNR $= \frac{\rho}{\sigma_{\mathrm{n}}^2}$. For fairness, the same total power constraint is enforced on all precoding algorithms. Finally, all reported results are averaged over 1000 random channel realizations.

A. SPECTRAL EFFICIENCY EVALUATION

We first investigate the spectral efficiency with different algorithms when perfect channel state information (CSI) is considered. To reduce the energy cost of the mmWave MIMO

$$\begin{aligned}
&\frac{1}{K}\sum_{k=1}^{K}\log_2\det\Big(\mathbf{I}+\frac{\rho\mu^2}{N_{\mathrm{s}}\sigma_{\mathrm{n}}^2}\mathbf{H}[k]\mathbf{F}_{\mathrm{RF}}\mathbf{F}_{\mathrm{RF}}^H\mathbf{H}[k]^H\Big)\\
&\quad=\frac{1}{K}\sum_{k=1}^{K}\log_2\det\big(\mathbf{Q}_j[k]\big)+\frac{1}{K}\sum_{k=1}^{K}\log_2\det\Big(\mathbf{I}+\frac{\rho\mu^2}{N_{\mathrm{s}}\sigma_{\mathrm{n}}^2}\mathbf{f}_j^H\mathbf{H}^H[k]\mathbf{Q}_j^{-1}[k]\mathbf{H}[k]\mathbf{f}_j\Big)\\
&\quad\overset{(b)}{\le}\frac{1}{K}\sum_{k=1}^{K}\log_2\det\big(\mathbf{Q}_j[k]\big)+\log_2\det\Big(1+\frac{\rho\mu^2}{N_{\mathrm{s}}\sigma_{\mathrm{n}}^2}\mathbf{f}_j^H\big(\frac{1}{K}\sum_{k=1}^{K}\mathbf{H}^H[k]\mathbf{Q}_j^{-1}[k]\mathbf{H}[k]\big)\mathbf{f}_j\Big).
\end{aligned} \tag{32}$$

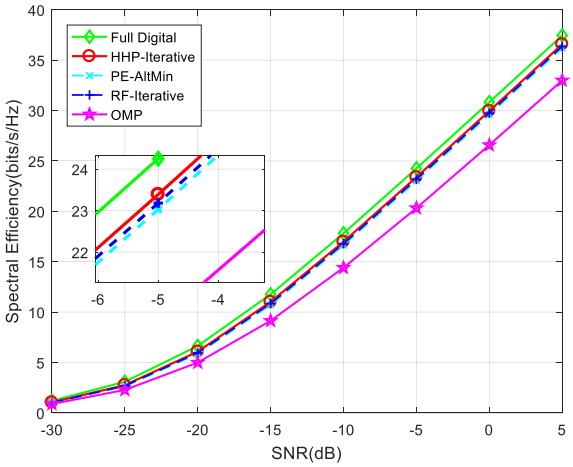

FIGURE 2. Spectral efficiency achieved by different precoding algorithms when $N_{RF} = N_s = 4$.

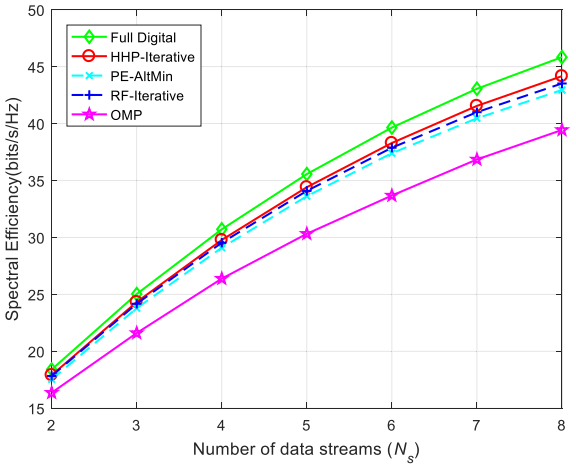

FIGURE 3. Spectral efficiency achieved by different precoding algorithms given $N_{RF} = N_s$ and SNR = 0 dB.

system, we assume that the number of RF chains is equal to that of the data streams, i.e., $N_{RF}^{t} = N_{RF}^{r} = N_{RF} = N_s$. In addition, for the proposed and reference algorithms, we set the number of iterations to three, which will be verified in the subsequent simulation. As shown in Fig. 2, the optimal digital precoder and OMP algorithm [13] are plotted as upper and lower baselines of performance, respectively. For comparison purposes, we also plot the spectral efficiency of the RF-Iterative algorithm [19] and PE-AltMin algorithm [20]. In this case, the proposed HHP-Iterative algorithm can achieve the near-optimal performance in Fig. 2. This implies that the proposed algorithm is superior to other algorithms, even though the RF chains are limited.

For addition simulation validation, we compare the performance of different precoding algorithms for different N_s in Fig. 3. As the number of data streams increases, the HHP-Iterative algorithm can more accurately access to the optimal digital precoder than the reference algorithms.

To examine the convergence of the proposed HHP-Iterative algorithm, we show the spectral efficiency versus number of iterations in Fig. 4. We see that the HHP-Iterative algorithm converge faster than the RF-Iterative algorithm, which has significant application value for practical scenario. In particular, when the number of iterations is two, the proposed algorithm can achieve satisfactory performance. Moreover, our proposed algorithm is outperform the RF-Iterative and PE-AltMin algorithms over the whole number of iteration range in consideration. Moreover, according to Fig. 4, it is reasonable to set the number of iterations to three for the previous parameter setting.

When the imperfect CSI is considered, we evaluate the performance of the proposed HHP-Iterative algorithm. Then, we denote the estimated channel as $\hat{\mathbf{H}}$, which can be modeled as

$$\hat{\mathbf{H}} = \tau \mathbf{H} + \sqrt{1-\tau^2}\mathbf{E}, \tag{34}$$

where $\tau \in [0, 1]$ represents the accuracy of channel estimation, and $\mathbf{E}$ is the error matrix which follows i.i.d. $\mathcal{CN}(0, 1)$.

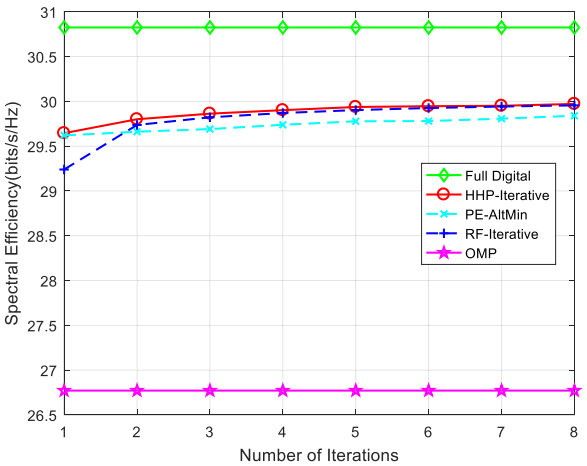

FIGURE 4. Spectral efficiency achieved by different precoding algorithms given $N_{RF} = N_s = 4$ and SNR = 0 dB.

When we consider the imperfect CSI with different τ scenarios, in Fig. 5, we show the spectral efficiency of the HHP-Iterative algorithm for an $N_r \times N_t = 36 \times 144$, $N_{RF} = N_s = 4$ mmWave MIMO system. Obviously, the performance of HHP-Iterative algorithm increases when τ becomes larger. Moreover, it can be seen that the proposed HHP-Iterative algorithm is insensitive to the CSI accuracy. For example, when $\tau = 0.9$, the performance of HHP-Iterative quickly get close to that in the perfect CSI case. In addition, considering the case of low CSI accuracy (i.e., $\tau = 0.5$), the HHP-Iterative algorithm with imperfect CSI can still achieve acceptable performance.

B. SYMBOL ERROR RATE EVALUATION

In this part, we study the symbol error rate (SER) with different algorithms when the number of RF chains is equal to that of the data streams in mmWave MIMO systems. In addition, the modulation scheme is 16QAM for all algorithms. As shown in Fig. 6, we observe that the SER of pro-

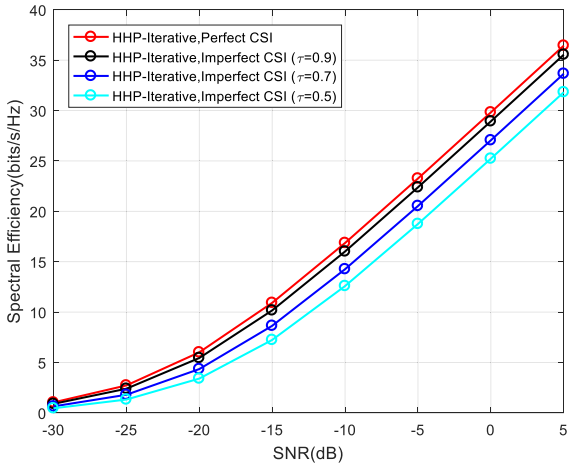

FIGURE 5. Impact of imperfect CSI on the proposed HHP-Iterative algorithm when $N_{RF} = N_S = 4$.

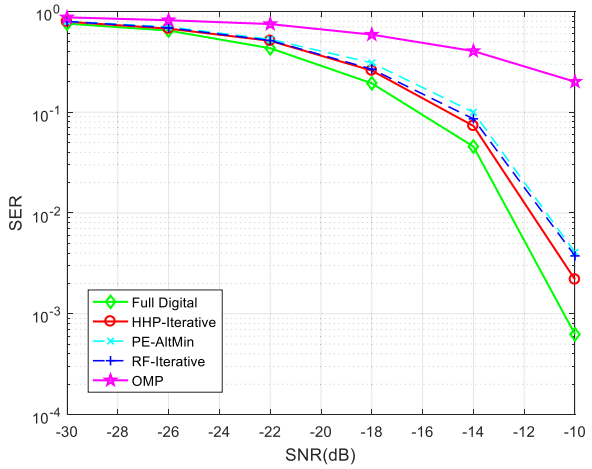

FIGURE 6. Symbol error rate achieved by different precoding algorithms when $N_{RF} = N_S = 4$.

posed HHP-Iterative is lower than that of OMP, PE-AltMin and RF-Iterative algorithms over the whole SNR range in consideration.

C. HYBRID PRECODER IN WIDEBAND MMWAVE MIMO-OFDM SYSTEMS

In this subsection, we show the performance of proposed HHP-Iterative algorithm for wideband mmWave MIMO-OFDM systems. Similarly to [20], we assume that the number of subcarriers is $K = 128$. In this case, we plot the spectral efficiency achieved by the HHP-Iterative algorithm in Fig. 7, which also includes the OMP and PE algorithm for comparison. Obviously, the HHP-Iterative algorithm can also achieve near-optimal performance in wideband mmWave MIMO-OFDM systems. When the number of RF chains increases, the HHP-Iterative algorithm can achieve better performance than the reference algorithms. It can be seen that the result is the same as that in narrowband systems. Therefore, in wideband mmWave systems, the additional OFDM processing on the digital precoder has no effect on spectral efficiency.

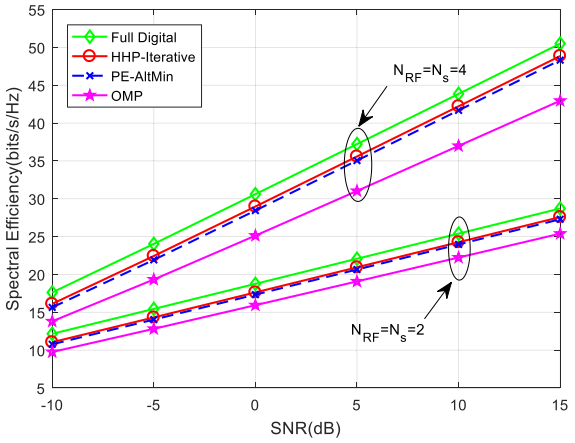

FIGURE 7. Spectral efficiency achieved by different precoding algorithms in mmWave MIMO-OFDM systems when $N_{RF} = N_S = 4$.

To sum up, the proposed HHP-Iterative algorithm can achieve satisfactory performance, both in narrowband and wideband OFDM systems.

VII. CONCLUSION

In this paper, we investigate the hybrid precoder and combiner in mmWave MIMO systems. Based on hierarchical strategy, we simplify the design of hybrid precoder. In addition, a novel iterative algorithm is proposed to optimize the analog precoder, and then the optimal digital precoder is computed based on the obtained analog precoder. After that, according to the same hierarchical strategy as hybrid precoder, we design the hybrid combiner. For the practical implementation, the proposed hybrid precoder design can be used to mmWave MIMO-OFDM systems. Simulation results and mathematical analysis show that the proposed algorithm can achieve near-optimal performance with low complexity, both in narrowband and wideband OFDM systems. In the future, we will further consider hybrid precoder design for mmWave multiuser MIMO systems.

APPENDIX A
PROOF OF (18)

According to (17), the objective function is expanded as

$$\begin{aligned}&\mathbf{f}_j^H \mathbf{M}_j \mathbf{f}_j \\ &= \left|\mathbf{f}_j(i)\right|^2 \mathbf{M}_j(i,i) + \mathbf{f}_j^H(-i)\mathbf{M}_j(-i,-i)\mathbf{f}_j(-i) \\ &\quad + 2\Re\left\{\mathbf{f}_j^H(i)\mathbf{M}_j^H(-i,i)\mathbf{f}_j(-i)\right\}, \end{aligned} \tag{35}$$

where $\mathbf{f}_j(-i)$ is a vector excluding the i-th element $\mathbf{f}_j(i)$ of $\mathbf{f}_j$ and $\mathbf{M}_j(-i,-i)$ is a matrix excluding the i-th row and i-th column of $\mathbf{M}_j$. Obviously, when we design $\mathbf{f}_j(i)$, the first two terms of (35) can be treated as constants. Therefore, the corresponding problem can be written as

$$\begin{aligned}&\arg\max_{\mathbf{f}_j(i)} \ \Re\left\{\mathbf{f}_j^H(i)\sum_{\substack{u=1\\u\neq i}}^{N_t}\mathbf{M}_j^H(u,i)\mathbf{f}_j(u)\right\}. \\ &\text{s.t. } |\mathbf{f}_j(i)| = 1, \quad \forall i. \end{aligned} \tag{36}$$

The optimal solution can be easily obtained as

$$\mathbf{f}_j^{\text{opt}}(i) = \psi \left\{ \sum_{\substack{u=1 \\ u \neq i}}^{N_\text{t}} \mathbf{M}_j^H(u,i)\mathbf{f}_j(u) \right\}. \tag{37}$$

APPENDIX B
PROOF OF (20)

We first consider the matrix $\mathbf{Q}_j$, which is necessary to compute the matrix $\mathbf{M}_j$. According to (13), $\mathbf{Q}_j$ can be rewritten as

$$\begin{aligned}
\mathbf{Q}_j &= \mathbf{I} + \frac{\rho\mu^2}{N_\text{s}\sigma_\text{n}^2}\mathbf{H}(\mathbf{F}_\text{RF})_{-j}(\mathbf{F}_\text{RF})_{-j}^H\mathbf{H}^H \\
&= \mathbf{I} + \frac{\rho\mu^2}{N_\text{s}\sigma_\text{n}^2}\mathbf{H}\big(\left[(\mathbf{F}_\text{RF})_{-j}\ \mathbf{f}_j\right]\left[(\mathbf{F}_\text{RF})_{-j}\ \mathbf{f}_j\right]^H \\
&\quad - \mathbf{f}_j\mathbf{f}_j^H\big)\mathbf{H}^H \\
&= \mathbf{I} + \frac{\rho\mu^2}{N_\text{s}\sigma_\text{n}^2}\mathbf{H}\mathbf{F}_\text{RF}\mathbf{F}_\text{RF}^H\mathbf{H}^H - \frac{\rho\mu^2}{N_\text{s}\sigma_\text{n}^2}\mathbf{H}\mathbf{f}_j\mathbf{f}_j^H\mathbf{H}^H.
\end{aligned} \tag{38}$$

Then, by using the Sherman-Morrison formula [30]

$$(\mathbf{X} + \mathbf{u}\mathbf{v}^H)^{-1} = \mathbf{X}^{-1} - \frac{\mathbf{X}^{-1}\mathbf{u}\mathbf{v}^H\mathbf{X}^{-1}}{1 + \mathbf{v}^H\mathbf{X}^{-1}\mathbf{u}}. \tag{39}$$

Thus, $\mathbf{Q}_j^{-1}$ can be written as

$$\begin{aligned}
\mathbf{Q}_j^{-1} &= \big(\mathbf{I} + \frac{\rho\mu^2}{N_\text{s}\sigma_\text{n}^2}\mathbf{H}\mathbf{F}_\text{RF}\mathbf{F}_\text{RF}^H\mathbf{H}^H - \frac{\rho\mu^2}{N_\text{s}\sigma_\text{n}^2}\mathbf{H}\mathbf{f}_j\mathbf{f}_j^H\mathbf{H}^H\big)^{-1} \\
&= \big(\mathbf{A} - \frac{\rho\mu^2}{N_\text{s}\sigma_\text{n}^2}\mathbf{H}\mathbf{f}_j\mathbf{f}_j^H\mathbf{H}^H\big)^{-1} \\
&= \mathbf{A}^{-1} + \frac{\frac{\rho\mu^2}{N_\text{s}\sigma_\text{n}^2}\mathbf{A}^{-1}\mathbf{H}\mathbf{f}_j\mathbf{f}_j^H\mathbf{H}^H\mathbf{A}^{-1}}{1 - \frac{\rho\mu^2}{N_\text{s}\sigma_\text{n}^2}\mathbf{f}_j^H\mathbf{H}^H\mathbf{A}^{-1}\mathbf{H}\mathbf{f}_j},
\end{aligned} \tag{40}$$

where the matrix $\mathbf{A} = \mathbf{I} + \frac{\rho\mu^2}{N_\text{s}\sigma_\text{n}^2}\mathbf{H}\mathbf{F}_\text{RF}\mathbf{F}_\text{RF}^H\mathbf{H}^H$. After that, $\mathbf{M}_j$ can be expressed as

$$\begin{aligned}
\mathbf{M}_j &= \mathbf{H}^H\mathbf{Q}_j^{-1}\mathbf{H} \\
&= \mathbf{H}^H\big(\mathbf{A}^{-1} + \frac{\frac{\rho\mu^2}{N_\text{s}\sigma_\text{n}^2}\mathbf{A}^{-1}\mathbf{H}\mathbf{f}_j\mathbf{f}_j^H\mathbf{H}^H\mathbf{A}^{-1}}{1 - \frac{\rho\mu^2}{N_\text{s}\sigma_\text{n}^2}\mathbf{f}_j^H\mathbf{H}^H\mathbf{A}^{-1}\mathbf{H}\mathbf{f}_j}\big)\mathbf{H} \\
&= \mathbf{H}^H\mathbf{A}^{-1}\mathbf{H} + \frac{\frac{\rho\mu^2}{N_\text{s}\sigma_\text{n}^2}\mathbf{H}^H\mathbf{A}^{-1}\mathbf{H}\mathbf{f}_j\mathbf{f}_j^H\mathbf{H}^H\mathbf{A}^{-1}\mathbf{H}}{1 - \frac{\rho\mu^2}{N_\text{s}\sigma_\text{n}^2}\mathbf{f}_j^H\mathbf{H}^H\mathbf{A}^{-1}\mathbf{H}\mathbf{f}_j} \\
&= \mathbf{B} + \frac{\frac{\rho\mu^2}{N_\text{s}\sigma_\text{n}^2}\mathbf{B}\mathbf{f}_j\mathbf{f}_j^H\mathbf{B}}{1 - \frac{\rho\mu^2}{N_\text{s}\sigma_\text{n}^2}\mathbf{f}_j^H\mathbf{B}\mathbf{f}_j},
\end{aligned} \tag{41}$$

where the matrix $\mathbf{B} = \mathbf{H}^H\mathbf{A}^{-1}\mathbf{H}$.

REFERENCES

[1] M. Xiao *et al.*, "Millimeter wave communications for future mobile networks," *IEEE J. Sel. Areas Commun.*, vol. 35, no. 9, pp. 1909–1935, Sep. 2017.

[2] S. Rangan, T. S. Rappaport, and E. Erkip, "Millimeter-wave cellular wireless networks: Potentials and challenges," *Proc. IEEE*, vol. 102, no. 3, pp. 366–385, Mar. 2014.

[3] W. Roh *et al.*, "Millimeter-wave beamforming as an enabling technology for 5G cellular communications: Theoretical feasibility and prototype results," *IEEE Commun. Mag.*, vol. 52, no. 2, pp. 106–113, Feb. 2014.

[4] J. G. Andrews *et al.*, "What will 5G be?" *IEEE J. Sel. Areas Commun.*, vol. 32, no. 6, pp. 1065–1082, Jun. 2014.

[5] A. Alkhateeb, J. Mo, N. Gonzalez-Prelcic, and R. W. Heath, Jr., "MIMO precoding and combining solutions for millimeter-wave systems," *IEEE Commun. Mag.*, vol. 52, no. 12, pp. 122–131, Dec. 2014.

[6] Z. Pi and F. Khan, "An introduction to millimeter-wave mobile broadband systems," *IEEE Commun. Mag.*, vol. 49, no. 6, pp. 101–107, Jun. 2011.

[7] T. S. Rappaport *et al.*, "Millimeter wave mobile communications for 5G cellular: It will work!" *IEEE Access*, vol. 1, pp. 335–349, May 2013.

[8] S. Han, C.-L. I, Z. Xu, and C. Rowell, "Large-scale antenna systems with hybrid analog and digital beamforming for millimeter wave 5G," *IEEE Commun. Mag.*, vol. 53, no. 1, pp. 186–194, Jan. 2015.

[9] R. Méndez-Rial, C. Rusu, N. González-Prelcic, A. Alkhateeb, and R. W. Heath, Jr., "Hybrid MIMO architectures for millimeter wave communications: Phase shifters or switches?" *IEEE Access*, vol. 4, pp. 247–267, 2016.

[10] R. W. Heath, Jr., N. González-Prelcic, S. Rangan, W. Roh, and A. M. Sayeed, "An overview of signal processing techniques for millimeter wave MIMO systems," *IEEE J. Sel. Topics Signal Process.*, vol. 10, no. 3, pp. 436–453, Apr. 2016.

[11] O. E. Ayach, R. W. Heath, Jr., S. Abu-Surra, S. Rajagopal, and Z. Pi, "Low complexity precoding for large millimeter wave MIMO systems," in *Proc. IEEE Int. Conf. Commun. (ICC)*, Jun. 2012, pp. 3724–3729.

[12] W.-L. Hung, C.-H. Chen, C.-C. Liao, C.-R. Tsai, and A.-Y. A. Wu, "Low-complexity hybrid precoding algorithm based on orthogonal beamforming codebook," in *Proc. IEEE Workshop Signal Process. Syst. (SiPS)*, Oct. 2015, pp. 1–5.

[13] O. El Ayach, S. Rajagopal, S. Abu-Surra, Z. Pi, and R. W. Heath, Jr., "Spatially sparse precoding in millimeter wave MIMO systems," *IEEE Trans. Wireless Commun.*, vol. 13, no. 3, pp. 1499–1513, Mar. 2014.

[14] H. Seleem, A. I. Sulyman, and A. Alsanie, "Hybrid precoding-beamforming design with Hadamard RF codebook for mmWave large-scale MIMO systems," *IEEE Access*, vol. 5, pp. 6813–6823, 2017.

[15] Y.-Y. Lee, C.-H. Wang, and Y.-H. Huang, "A hybrid RF/baseband precoding processor based on parallel-index-selection matrix-inversion-bypass simultaneous orthogonal matching pursuit for millimeter wave MIMO systems," *IEEE Trans. Signal Process.*, vol. 63, no. 2, pp. 305–317, Jan. 2015.

[16] C.-C. Yeh, K.-N. Hsu, and Y.-H. Huang, "A low-complexity partially updated beam tracking algorithm for mmWave MIMO systems," in *Proc. IEEE Global Conf. Signal Inf. Process. (GlobalSIP)*, Dec. 2016, pp. 748–752.

[17] W. Ni, X. Dong, and W. S. Lu, "Near-optimal hybrid processing for massive MIMO systems via matrix decomposition," *IEEE Trans. Signal Process.*, vol. 65, no. 15, pp. 3922–3933, Aug. 2017.

[18] J.-C. Chen, "Hybrid beamforming with discrete phase shifters for millimeter-wave massive MIMO systems," *IEEE Trans. Veh. Technol.*, vol. 66, no. 8, pp. 7604–7608, Aug. 2017.

[19] F. Sohrabi and W. Yu, "Hybrid digital and analog beamforming design for large-scale antenna arrays," *IEEE J. Sel. Topics Signal Process.*, vol. 10, no. 3, pp. 501–513, Apr. 2016.

[20] X. Yu, J.-C. Shen, J. Zhang, and K. B. Letaief, "Alternating minimization algorithms for hybrid precoding in millimeter wave MIMO systems," *IEEE J. Sel. Topics Signal Process.*, vol. 10, no. 3, pp. 485–500, Apr. 2016.

[21] Z. Wang, M. Li, Q. Liu, and A. L. Swindlehurst, "Hybrid precoder and combiner design with low-resolution phase shifters in mmWave MIMO systems," *IEEE J. Sel. Topics Signal Process.*, vol. 12, no. 2, pp. 256–269, May 2018.

[22] M. Li, Z. Wang, X. Tian, and Q. Liu, "Joint hybrid precoder and combiner design for multi-stream transmission in mmWave MIMO systems," *IET Commun.*, vol. 11, no. 17, pp. 2596–2604, 2017.

[23] A. Alkhateeb and R. W. Heath, Jr., "Frequency selective hybrid precoding for limited feedback millimeter wave systems," *IEEE Trans. Commun.*, vol. 64, no. 5, pp. 1801–1818, May 2016.

[24] F. Sohrabi and W. Yu, "Hybrid analog and digital beamforming for mmWave OFDM large-scale antenna arrays," *IEEE J. Sel. Areas Commun.*, vol. 35, no. 7, pp. 1432–1443, Jul. 2017.

[25] A. Goldsmith, S. A. Jafar, N. Jindal, and S. Vishwanath, "Capacity limits of MIMO channels," *IEEE J. Sel. Areas Commun.*, vol. 21, no. 5, pp. 684–702, Jun. 2003.
[26] V. Raghavan and A. M. Sayeed, "Sublinear capacity scaling laws for sparse MIMO channels," *IEEE Trans. Inf. Theory*, vol. 57, no. 1, pp. 345–364, Jan. 2011.
[27] N. Li, Z. Wei, H. Yang, X. Zhang, and D. Yang, "Hybrid precoding for mmWave massive MIMO systems with partially connected structure," *IEEE Access*, vol. 5, pp. 15142–15151, 2017.
[28] J. Lee and Y. H. Lee, "AF relaying for millimeter wave communication systems with hybrid RF/baseband MIMO processing," in *Proc. IEEE Int. Conf. Commun. (ICC)*, Jun. 2014, pp. 5838–5842.
[29] X. Wu, N. C. Beaulieu, and D. Liu, "On favorable propagation in massive MIMO systems and different antenna configurations," *IEEE Access*, vol. 5, pp. 5578–5593, 2017.
[30] G. H. Golub and C. F. van Loan, *Matrix Computations*, vol. 3. Baltimore, MD, USA: The Johns Hopkins University Press, 2012.

RAN ZHANG received the bachelor's degree in Internet of Things engineering from the Hebei University of Engineering, in 2016. She is currently pursuing the Ph.D. degree in communication engineering with the Beijing University of Posts and Telecommunications. Her research interests include millimeter wave communications, massive MIMO, and hybrid precoding.

WEIXIA ZOU received the B.S. degree in electric traction and drive control from Tongji University, in 1994, the M.S. degree in circuits and systems from Shandong University, in 2002, and the Ph.D. degree in communication and information system from the Beijing University of Posts and Telecommunications, Beijing, China, in 2006, where she is currently an Associate Professor. Her current research is in the new technologies of short-range wireless communication and 60 GHz.

YE WANG received the B.Eng. degree in electronic science and technology from Tianjin University, Tianjin, China, in 2010, and the M.A.Eng. degree in telecommunication engineering from the University of Melbourne, Melbourne, Australia, in 2013. He is currently pursuing the Ph.D. degree in information and communication engineering with the Beijing University of Posts and Telecommunications, Beijing. His research interests include millimeter wave communications, optimization algorithms, and massive MIMO systems.

MINGYANG CUI was born in Henan, China, in 1993. He is currently pursuing the Ph.D. degree in engineering of telecommunication with the Beijing University of Posts and Telecommunications. His research interests include millimeter wave communication and performance optimization in massive MIMO systems.